Numerical Analysis of Metal Transfer in Gas Metal Arc Welding under Modified Pulsed Current Conditions

G. Wang

P.G. Huang

Department of Mechanical Engineering

Y.M. Zhang

Center for Manufacturing and Department of Electrical and Computer Engineering

University of Kentucky

Abstract

A method has been proposed to pulsate current in gas metal arc welding (GMAW) to achieve a specific type of desirable and repeatable metal transfer modes, i.e., one drop per pulse (ODPP) mode. It uses a peak current lower than the transition current to prevent accidental detachment and takes advantage of the downward momentum of the droplet oscillation droplet to enhance the detachment. A numerical model with advanced computational fluid dynamics (CFD) techniques, such as a two-step projection method, volume of fluid (VOF) method and continuum surface force (CSF) model, iswas used to carry out the simulation for metal transfer process. The Gauss-type current density distribution wasis assumed as the boundary condition for the calculation of the electromagnetic force. The calculations wereare conducted to demonstrate the effectiveness of the proposed method in achieving the desired metal transfer process in comparison with conventional pulsed current GMAW. Also, the critical condition for effective utilization of this proposed method wasis identified by numerical simulation. Comparison showsed good agreement between calculation and experimental results.

1.Introduction

In gas metal arc welding (GMAW), several different modes of the metal transfer have been classified [1]. At low current, the globular transfer occurs if the arc length is sufficient. The drops grow at the tip of the electrode with a classic pendant drop

shape, due to the competition between gravity and surface tension in the presence of relatively small electromagnetic forces. The large drops with diameter much greater than the diameter of the electrode are detached primarily by the gravity. When the welding current increases, the electromagnetic force becomes dominant droplet force so that small drops with diameter equal or less than the diameter of the electrode can be detached. This is referred to as the spray transfer mode. It is found that there is an abruptness transition in the current which divides the globular and spray transfer modes. This current or current range is referred to as the transition current. High irregularity in the drop detachment frequency and the drop size occurs in the middle of the transition current range [2-4].

Globular transfer mode typically causes significant spatters and poor welding quality [5]. Its application in production is rare. The spray transfer mode takes advantage over the globular mode by its regular detachment, directional droplet transfer and low spatters [3]. However, spray transfer is only achieved at high current, which causes a thermal load too high to apply to thin sectioned or heat-sensitive materials. In an effort to overcome this difficulty, pulsed current GMAW was introduced in 1962 [6]. By using a pulsed current, a controlled spray transfer mode can be achieved at low average current, which typically results in globular transfer. To further achieve the desirable one drop per pulse (ODPP) mode which characterizes a stable, periodical, and controllable metal transfer process, the necessary conditions were investigated in a number of works [7-18]. To this end, Ueguri [9] suggested the peak current should be set above a critical current while Amin [10] identified this critical current as the transition current between the globular

and spray transfer mode. Quintino [11-12] and Smati [13] showed the peak duration should be increased to get ODPP when the peak current decreases. The work of Kim [15-17] and his associates pointed out that there wasis a range of operational parameters within which one droplet wasis transferred per current pulse. This wasis further proved by the work conducted by Nemchinsky [18].

Recently, a novel active control technology has been proposed by Zhang *et al*., E and his associates [7-8] in order to achieve ODPP. The drop is detached by the combination of the downward momentum of the drop oscillation and the increased electromagnetic force, which is induced by an exciting pulse and a detaching pulse, respectively. The synchronization between the downward momentum and the increase of the detaching electromagnetic force is referred to as phase match. The phase match between the downward movement and increased current must be satisfied to ensure ODPP. This method introduces large amounts of additional welding parameters, which make it difficult to select optimum combinations of parameters for a wide range of welding conditions. A trial-and-error method wasis used to determine these parameters experimentally. However, this empirical approach is very time consuming.

A theoretical description of the metal transfer in GMAW can provide a better understanding of the technology's mechanism and a better means to determine the optimum operation parameters. Some numerical studies have been done for constant and for traditional pulsed current GMAW [15-24]. Such studies develop from the earliest static models to the dynamic models. In this work, a transient two-dimensional model developed based on RIPPLE [25] wasis used to simulate the

droplet formation, detachment, and transport in GMAW. The transient shape of the droplet wasis calculated using the fractional volume of fluid (VOF) method [26]. The continuum surface force (CSF) model [27] used here simplifies the calculation of surface tension and enables accurate modeling of fluid flows driven by surface forces. The electromagnetic force, which wasis generated by the welding current, wasis calculated by assuming Gauss-type current density distribution over the free surface of the droplet.

2.Proposed approach in modified pulsed current GMAW

In conventional pulsed GMAW using pulse waveform as shown in Figure 1(a), the drop is detached by the combination of the gravitational force and electromagnetic force. The detachment of a drop is still a natural detachment process. Under the current lower than the transition current, a natural detachment can occur only when the droplet is significantly larger than the diameter of the electrode. Hence, the peak current I_p must be higher than the transition current in order to guarantee that the droplet naturally detaches with a size similar to the diameter of the electrode [9,10]. On the other hand, the use of a peak current higher than the transition current frequently brings accidental detachment, which causes multiple-droplets-per-pulse (MDPP).

To guarantee ODPP with the droplet size similar to the diameter of electrode, while the peak current is lower than the transition current to prevent the accidental detachment, a novel active control technology has been recently proposed [8]. In this modified pulsed current GMAW, a pulse repetition cycle is composed of two periods: growth period and detachment period as shown in Figure 1(b). To detach one drop in every pulse cycle is still referred to as ODPP mode with emphasizing on its periodical and controllable characteristic. An exciting pulse edge is applied at the end of the growth period when the current is switched to the base level so that a sudden change in electromagnetic force is imposed to the droplet. As a result, an oscillation of the droplet is introduced. After a period T_{b2} as shown in Figure 1(b), a detaching pulse is applied. The downward momentum of the oscillating droplet enhances detachment and eliminates the need for a higher current to detach the droplet. (The detachment of the droplet is no longer a natural transition in this proposed approach but result of control.) Hence, the peak current can be lower than the transition current to detach the droplet while at the same time accidental detachment is prevented. Because the current used in the growth period is lower than the transition current and should not be qualified as a pulse as classically defined, the achieved "one drop in one pulse cycle" metal transfer, which has similar periodical and controllable characteristics as ODPP, is referred to as modified ODPP mode or simply ODPP for convenience of discussion.

From the parameters of modified pulsed current GMAW shown in Figure 1(b),

$$T_b = T_{b1} + T_{b2} \tag{1}$$

$$T_p = T_{p1} + T_{p2} \tag{2}$$

$$T = T_{b1} + T_{b2} + T_{p1} + T_{p2} = T_b + T_p = 1/f \tag{3}$$

$$I_{avg} = (I_p * T_{p1} + I_p * T_{p2} + I_b * T_{b1} + I_b * T_{b2}) / T = (I_p * T_p + I_b * T_b) * f \tag{4}$$

Where f is the pulse frequency, I_{avg} is the average current, I_p is the peak current, I_b is the background current, T_p and T_b represent the peak and base duration. Any four of them are given as preset parameters. The other two parameters can be determined accordingly. The waveform of the welding current can be changed by the adjustment of T_{p1}, T_{p2}, T_{b1}

and T_{b2} without change of the preset parameters. By properly choosing the waveform of the welding current, the proposed method takes advantage of synchronization between the downward momentum of the droplet oscillation and the detaching pulse to realize ODPP. The synchronization between the downward momentum and the increase of the detaching electromagnetic force is referred to as phase match.

Experiments have demonstrated the effectiveness of the proposed approach. But a significant limitation of the developed control system found by experiment is the use of a high-cost imaging system, which monitors the oscillating droplet to guarantee the phase match. Numerical simulations can provide a better understanding of the mechanism of this process and means to determine the optimum operation parameters.

3.Numerical Schemes

The numerical schemes used are based on a finite difference solution of a coupled set of partial differential equations governing unsteady incompressible fluid flow

$$\nabla \cdot \vec{v} = 0 \tag{5}$$

$$\rho \frac{D\vec{v}}{Dt} = -\nabla p + \nabla \cdot \vec{\tau} + \vec{F}_b \tag{6}$$

Where $\vec{v}$ is the velocity, ρ is the fluid density, p is the scalar pressure, $\vec{\tau}$ is the viscous stress tensor, and $\vec{F}_b$ is body force, which includes the gravitational force and the electromagnetic force. The two-step projection method [25] was used asis the basic algorithm for solving this set of partial differential equations. The transient shape of the droplet wasis calculated using the fractional volume of fluid (VOF)[26] method. The free surface profile is reconstructed by employing the function $F(\vec{x},t)$, which represents the fluid volume ratio of each cell. The function F takes the value of unity

for the cell filled with the fluid and zero for the empty cell. For incompressible flow, the VOF function might be regarded as the normalization $F(\vec{x},t) = \rho(\vec{x},t) / \rho_f$ **, where** ρ_f **is the constant fluid density. The discontinuity in** F **is a Lagrangian invariant, propagating according to**

$$\frac{dF}{dt} = \frac{\partial F}{\partial t} + (\vec{v} \cdot \nabla) F = 0 \tag{7}$$

Therefore, equation (7) implies that the function F should be solved simultaneously with equation (5) and (6). The surface tension of free surfaces is modeled as a localized volume force derived from the continuum surface force (CSF) model [27]. The surface tension with volume form $\vec{F}_{sv}(\vec{x}) = \sigma\kappa(\vec{x})\nabla F(\vec{x}) g(\vec{x})$ can be easily counted by applying an extra body force term in the momentum equation (6), Where σ, κ and g are surface tension coefficient, local free surface curvature and optional function respectively. The electromagnetic force, $\vec{F}_m = \vec{J} \times \vec{B}$, generated by the welding current should be also included in the body force in the momentum equation (6). $\vec{J}$ and $\vec{B}$ represent the current density and magnetic flux density respectively. The current density is calculated from the electric potential, which satisfies the Laplace equation by assuming the electric field is quasi-steady-state and the electrical conductivity is constant. The boundary conditions for solving the Laplace equation to determine the distributions of the potential and current density within the drop, and further influence the electromagnetic force are important. Since experimental data concerning the current distribution on the drop's surface are not available in the literature due to the difficulty of making such measurements in the arc next to the free surface, an assumption wasis made based on our pervious theoretical study

[24]. The current density on the drop surface cell (i, j) wasis assumed following a Gaussian distribution:

$$J_{sij} = I \cdot f(i,j) / \sum_{n} \left(S_{i,j} \cdot f(i,j) \right)$$
$$f(i,j) = \frac{1}{\sqrt{2\pi}} \exp(-\xi^2 / 2) \qquad (8)$$
$$\xi = \frac{X}{D}$$

Where J_{sij} represents the current density on the surface cell (i, j), I the welding current, $S_{i,j}$ the area of the free surface cell (i, j), Where X is the arc (curve) length on the drop surface between the lowest point on the drop and the free surface cell (i, j), and D is diameter of the electrode when the welding current is constant. It has been proved by our previous study [24] that the results calculated by using a Gaussian current density distribution show better agreement with the experimental data than the results based on other modeling such as constant or linear assumption.

When the initial and boundary conditions are given, the flow velocity, pressure and potential distribution and free surface profile can be calculated. Metal transfer process in GMAW with initial and boundary conditions are illustrated in Figure 2. Assumptions made here include: (1) the problem is axisymmetric, (2) the input velocity of molten metal is the same as the wire feed rate no matter the current in peak or base duration, (3) free slip at the solid boundaries, (4) the velocities of the surrounding gas are set to zero with pressure of atmospheric condition, (5) an isopotential line (Φ = 0) is set at the inlet section, (6) Gaussian current density distribution on the droplet surface.

As mentioned earlier, the proposed approach takes advantage of the downward momentum of the excited oscillation to reduce the current level for the droplet detachment and prevent accidental detachment. In order to guarantee the detachment and realize

ODPP, the phase match between the downward momentum and the detaching action is crucial. The proper selection of T_{b2}, time interval between the exciting pulse and detaching pulse, determines whether or not the phase match condition between the downward momentum and the detaching action can be met. Because of the importance of the time interval T_{b2}, a numerical solution wasis introduced here to determine it and guarantee phase match. Since the oscillation of droplet is induced by exciting pulse, the excited oscillation of the droplet is numerically simulated first. Based on analysis of the calculated results, the proper time interval is then determined to assure ODPP.

4. Results and Discussions

Calculations wereare performed based on the experimental work of Zhang *et al*., E and Kovacevic [8]. Simulations wereare carried out for stainless steel electrode with a diameter of 1.2 mm. The physical properties of the stainless steel electrode are listed in Table 1. A uniform computational mesh with a spacing of 0.1 mm in each coordinate direction wasis used. While the mesh spacing was varied between 0.08 mm to 0.16mm, it was found that the calculated results remain unchanged. All calculations wereare performed on a SGI-Origin-2100 workstation.

4.1 Problems in Traditional Single Pulsed GMAW

The calculations wereare performed for the metal transfer process under constant current to predict the transition current first. The wire feed rate wasis selected to be 70mm/s. Figure 3 shows the predicted average drop sizes detached at different welding currents. As the welding current increases, the metal transfer mode changes from the globular mode with a large drop detached to the spray mode with a small drop detached. There exists a narrow current range over which the transition from the globular transfer mode to the spray transfer mode occurs. The transition current range for the stainless steel electrode with diameter of 1.2mm is predicted from 220A to 230A. It agrees well with the experimental results.

Figure 4 shows the dynamic drop development and detachment processes under traditional single pulsed current GMAW. There are two cases presented here. In these two cases, the average current I_{avg} is set towith 100A, where the pulse frequency f is 30Hz, and base current I_b is set to 40A. According to experimental data taken from the work of

Zhang *et al*., E, and Walcott [7], the wire feed rate wasis selected as 110in/min (46.5mm/s) for an average current of 100A. In the first case, one drop multiple pulses (ODMP) occurs as shown in Figure 4(a) when the peak current I_p is 220A. This result supports the general idea that the peak current must be larger than the transition current in order to guarantee that the droplet detaches with a size similar to the diameter of electrode in conventional single pulsed GMAW. Also, the droplet oscillation introduced by current pulse can be easily visualized from the Figure 4(a). It shows the instantaneous profiles for droplet bouncing to the highest position right after every time current pulse drags it down. It is noted the time for the droplet to reach the highest position after peak current is increased with increasing mass of droplet. In other words, the frequency of droplet oscillation after current pulse is decreased with increase of droplet mass. In the second case, the use of a peak current higher than the transition current ($I_p = 250$ A) easily brings accidental detachment as shown in Figure 4(b). Metal transfer with undesired mMulti-drops per pulse (MDPP) occurs.

4.2 Modified Pulsed Current GMAW

4.2.1 Advantages for Modified Pulsed Current GMAW

By simply splitting the pulse used in the first case above into two parts and keeping all other parameters unchanged (Fig.5a), the modified pulsed current GMAW takes advantage of the phase match between the downward momentum of the oscillating droplet introduced by the exciting pulse and the increased electromagnetic force brought by the detaching pulse. The current level, which is required to detach a drop with a size similar to the diameter of the electrode, is reduced by introducing the downward momentum of the oscillating droplet. The Figure 5(b) shows the one drop per pulse achieved with a droplet size similar to the diameter of the electrode under the peak current which is lower than the transition current by using the modified pulsed current GMAW.

4.2.2 Parameter Diagnoses for Phase Match

As it can be observed in Figure 5, when the time interval between two pulses T_{b2} is 4ms, the ODPP is realized. However, if a shorter duration T_{b2} = 3ms or a longer duration T_{b2} = 5.5ms is used, the ODPP cannot be realized as shown in Figure 6. In the above two cases, the failure of ODPP is caused by the unsatisfied phase match condition. In the first case as shown in Figure 6(a), the time interval between exciting pulse and detaching pulse is too short to let the drop bounce to its highest position before the detaching pulse is addedpresence. Hence, the drop continues moving to the higher position during part of the period of detaching pulse application. The upward momentum of drop not only can't reinforce detaching process, but also offsets the electromagnetic force and makes drop detachment process more difficult. In the second case, the longer time interval between exciting pulse and detaching pulse allows the drop to reach its highest position and move long way down before the detaching pulse presence. The downward momentum of droplet is decreasing when the drop moves its way down from its highest position. The joint effect of the decreasing downward momentum and the increasing electromagnetic force is not large enough to detach the droplet. Phase match isas a necessary condition for the proposed approach to be effectivemust be satisfied. Phase match can be achieved by the proper selection of T_{b2}. It is expensivebecomes difficult to determine T_{b2} experimentally due to the use of the high-cost imaging system. But the diagnoses for phase match can be achieved efficiently through mathematic modelingnumerically. For determining the value of T_{b2} to To asensure the phase match, the calculation wasis carried out first to simulate the response of the droplet under the stimulus of the exciting pulse.

Figure 7 shows the calculated vertical coordinate development of the droplet tip under the application of anthe exciting pulse I_{p1}. The oscillation of the droplet wasis introduced by the exciting pulse. In order to realize the phase match and take advantage of the downward momentum of the oscillating droplet, it has been determined that the proper time to add the detaching pulse is when the vertical coordinate of the droplet tip reaches the highest point and begin to move downwardly. From Figure 7, it is identified that in this case the droplet recoilsing back to its highest point 4 ms after the pulse in this case. As mentioned previously, ODPP is realized when T_{b2} is set ats 4 ms. Also, Figure 8 shows ODPP is achieved when a shorter T_{b2} of 3.5ms or a longer T_{b2} of 4.7ms is adopted (instants for droplet detachment are marked with dots in figure). Hence, the value of T_{b2} is determined according to analysis of the simulation results. It is noted that there is a time range around the droplet tip reaching the highest point, over which the ODPP can be achieved when the detaching pulse is added. Also, the optimum value of T_{b2} using to reach phase match is determined by the frequency of droplet oscillation $f_{drop} = 1/T = \sqrt{\frac{k}{m}}$. The proper value of T_{b2} is increased with increasing mass of droplet as observed in Figure 4(a).

4.2.3 Comparison with Experiment

Figure 9 shows the comparison between the calculated result and experimental [12] data provided by Zhang *et al.*, E and Kovacevic when the proposed active metal transfer control wasis employed. The average currents were is set atwith 100A and 165A, respectively. The pulsetransfer frequency wasis 30Hz for 100A and 65Hz for 165A. According to experimental data taken from the work of Zhang et al., E, and Walcott [7], tThe wire feed speeds were set atis given as 110in/min (46.5mm/s) for 100A and 180in/min (76.2mm/s) for 165A. The waveform of the welding current is shown in Figure 9(a). It was modeled as a pulse cycle, which was composed of exciting pulse with peak current of 210A and detaching pulse with peak current of 230A. The peak duration for detaching pulse was set to 6ms while the time interval T_{b2} was set to 3ms. The base current was 40A. The other parameters can be determined accordingly for both cases. The calculated and measured vertical coordinate of the droplet tip increases with time as are shown in Figure 9(b) and, (c) respectively. The predicted results agree well with the experimental data. One drop per pulse cycle wascircle is realized under these two sets of conditionsdata provided by the experiment.

5 Conclusions

A novel pulsed current GMAW that has been proposed by experiment is simulated and analyzed by using advanced CFD techniques. The proposed method takes advantage of synchronization between the downward momentum of the oscillating drop and the increased electromagnetic force to realize a modified ODPP in GMAW. The robustness of the metal transfer process in GMAW provided by this technology is significantly improved in comparison with conventional pulsed GMAW process. The calculation not only shows the effectiveness of the proposed approach to achieve one drop per pulse cycle, but also provides an effective means to diagnose the optimum operation parameters and paves the way for make this new technique feasible in industry.

List of Illustrations

Fig. 3 The relationship between the detached drop sizes and welding currents

Fig. 4 Metal transfer processes under conventional pulsed current GMAW: (a) Drop profiles at peak current of 220A (b) Drop profiles at peak current of 250A

Fig. 5 Metal transfer process in modified pulsed current GMAW: (a) Current waveform (b) Droplet profiles

Fig. 6 Metal transfer processes with unsatisfied phase match condition: (a) Drop profiles under a shorter duration T_{b2} of 3ms (b) Drop profiles under a longer duration T_{b2} of 5.5ms

Fig. 7 The droplet response to exciting pulse: (a) Current waveform (b) Vertical coordinate of droplet tip

Fig. 8 Development for vertical coordinate of droplet tip in modified pulsed current GMAW: (a) ODPP at T_{b2} of 3.5ms (b) ODPP at T_{b2} of 4.7ms

Fig. 9 Comparison between the calculated results and experimental data: (a) Current waveforms (b) vertical coordinate of droplet tip from experiment (c) vertical coordinate of droplet tip from calculation

References

1. J.F. Lancaster: The Physics of Welding, 2nd ed., 1986, Pergamon Press, Oxford.
2. L.A. Jones, T.W. Eagar, and J.H. Lang: Welding J., 1998, vol. 77, pp. 135s-141s.
3. A. Lesnewich: Welding J., 1958, vol. 37, pp. 418s-425s.
4. S.W. Simpson, P. Zhu, and M. Rados: Proc. 42nd Nat. Weld. Conf., 1994, vol. 31, pp.1-8.
5. S.T. Eickhoff and T.W. Eagar: Welding J., 1990, vol. 69, pp. 382s-388s
6. J.C. Needham: Physics of Welding Arc, 1962, pp. 114-124.

7. Y.M. Zhang, Liguo E and B.L. Walcott: ASME Journal of Dynamic Systems, Measurement, and Control, 2002, vol.124, pp. 281-289.
8. Y.M. Zhang, Liguo E and R. Kovacevic: Welding J., 1998, vol. 77, pp. 388s-395s.
9. S. Ueguri, K. Hara and H. Komura: Welding J., 1985, vol. 64, pp. 242s-250s.
10. M. Amin: Metal Construction, 1983, vol. 15, pp. 272-278.
11. L. Quintino and C.J. Allum: Welding Met. Fabrication, 1984, vol. 4, pp. 126-129.
12. L. Quintino and C.J. Allum: Welding Met. Fabrication, 1984, vol. 3, pp. 85-89.
13. Z. Smati: Met. Construction, 1986, vol. 18, pp. 38-44.
14. N. Jacobsen: J. Phys. D, 1992, vol. 25, pp. 783-797.
15. Y.S. Kim: Ph.D thesis, 1989, MIT, Cambridge, MA.
16. Y.S. Kim and T.W. Eagar: Welding J., 1993, vol. 72, pp. 279s-287s.
17. S.K. Choi, C.D. Yoo and Y.S. Kim: J. Phys. D, 1998, vol. 31, pp. 207-215.
18. V.A. Nemchinsky: J. Phys. D, 1998, vol. 31, pp. 2797-2802.
19. C.J. Allum: J. Phys. D, 1985, vol. 18, pp. 1447-68.
20. S.W. Simpsom, and P. Zhu: J. Phys. D, 1995, vol. 28, pp. 1594-600.
21. J. Haidar: J. Phys. D, 1998, vol. 31, pp. 1233-44.
22. H.G. Fan, and R. Kovacevic: Metall. Mater. Trans. B, 1999, vol. 30B, pp. 791-801.
23. S.K. Chio, Y.S. Kim, and C.D. Yoo: J. Phys. D, 1999, vol. 32, pp. 326-34.
24. G. Wang, P.G. Huang and Y.M. Zhang: Metall. Mater. Trans. B, 2003, vol. 34B, pp.345-353
25. D.B. Kothe, R.C. Mjolsness, and M.D. Torrey: RIPPLE, Los Alamos National Laboratory, 1994, LA-12007-MS.
26. C.W. Hirt, and B.D. Nichols: J. Comp. Phys., 1981, vol. 39, pp. 201-225.

27. J.U. Brackbill, D.B. Kothe, and C. Zemach: J. Comp. Phys., 1992, vol. 100, pp. 335-54.

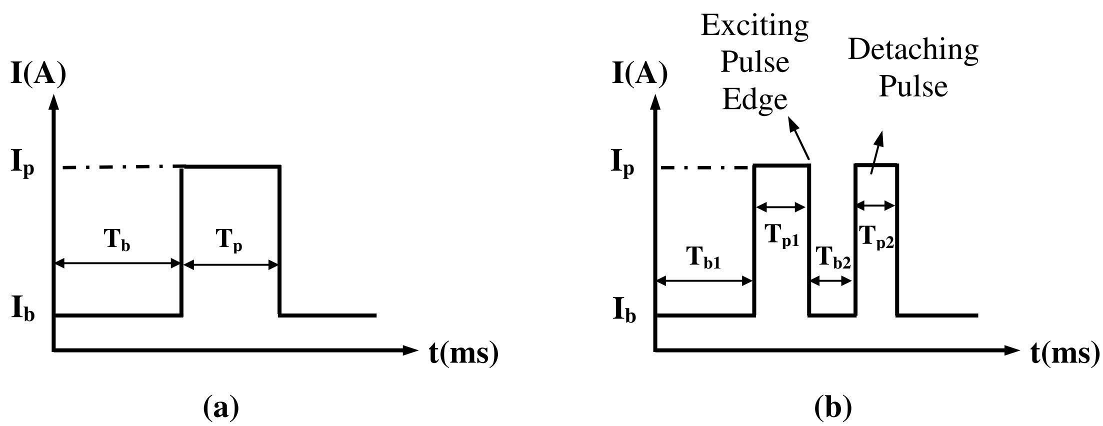

Figure 1

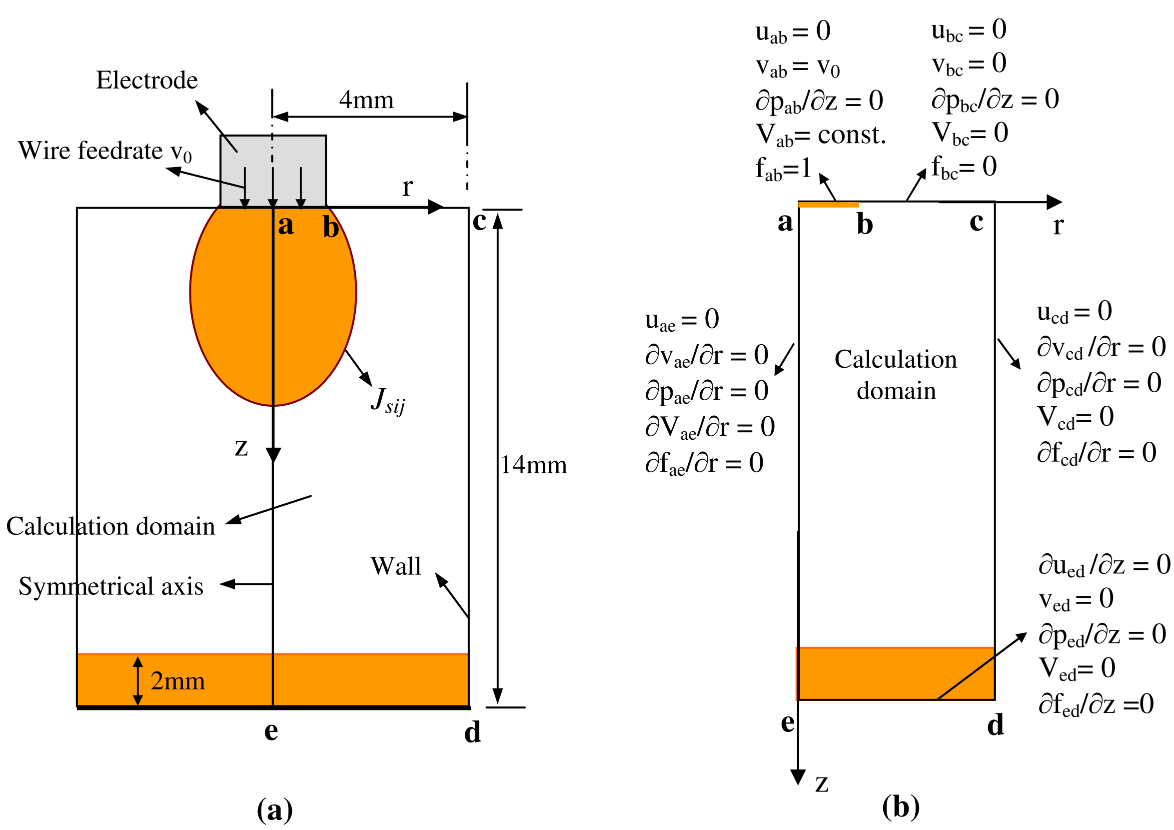

Figure 2

Table 1. Material Properties of the Electrode

Mass density ρ	7860 kg/m^3
Kinematic viscosity ν	2.8×10^{-7} m^2/s
Surface tension coefficient γ	1.2 N/m
Electrical Conductivity σ	8.54×10^5 mho/m
Permeability μ	$4\pi \times 10^{-7}$ H/m

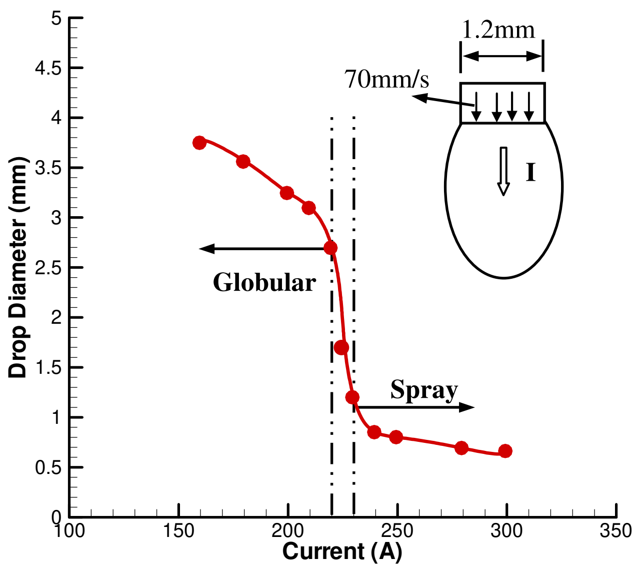

Figure 3

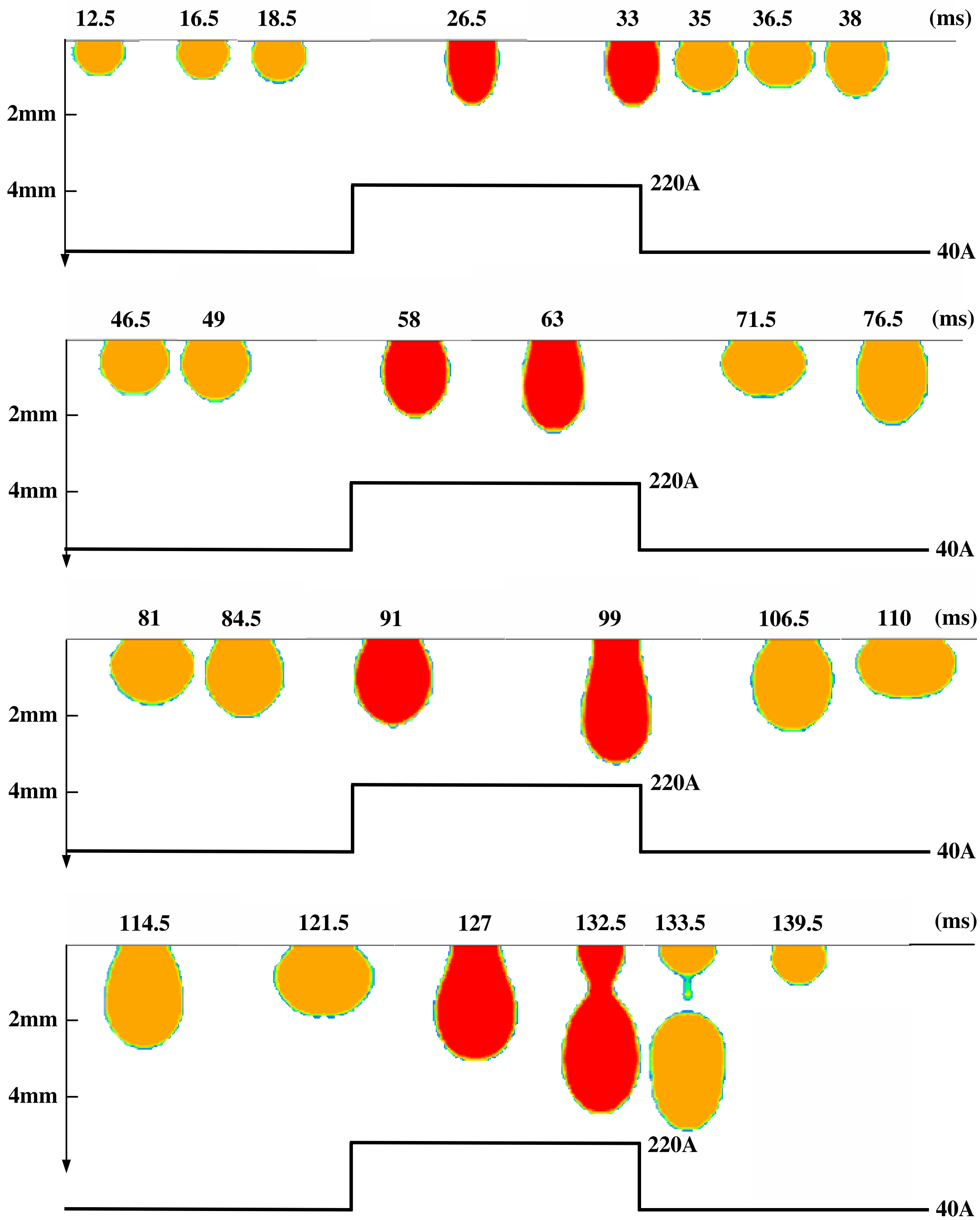

12.5
16.5
18.5
26.5
33
35
36.5
38
(ms)
2mm
4mm
220A
40A
46.5
49
58
63
71.5
76.5
(ms)
2mm
4mm
220A
40A
81
84.5
91
99
106.5
110
(ms)
2mm
4mm
220A
40A
114.5
121.5
127
132.5
133.5
139.5
(ms)
2mm
4mm
220A
40A

Figure 4(a)

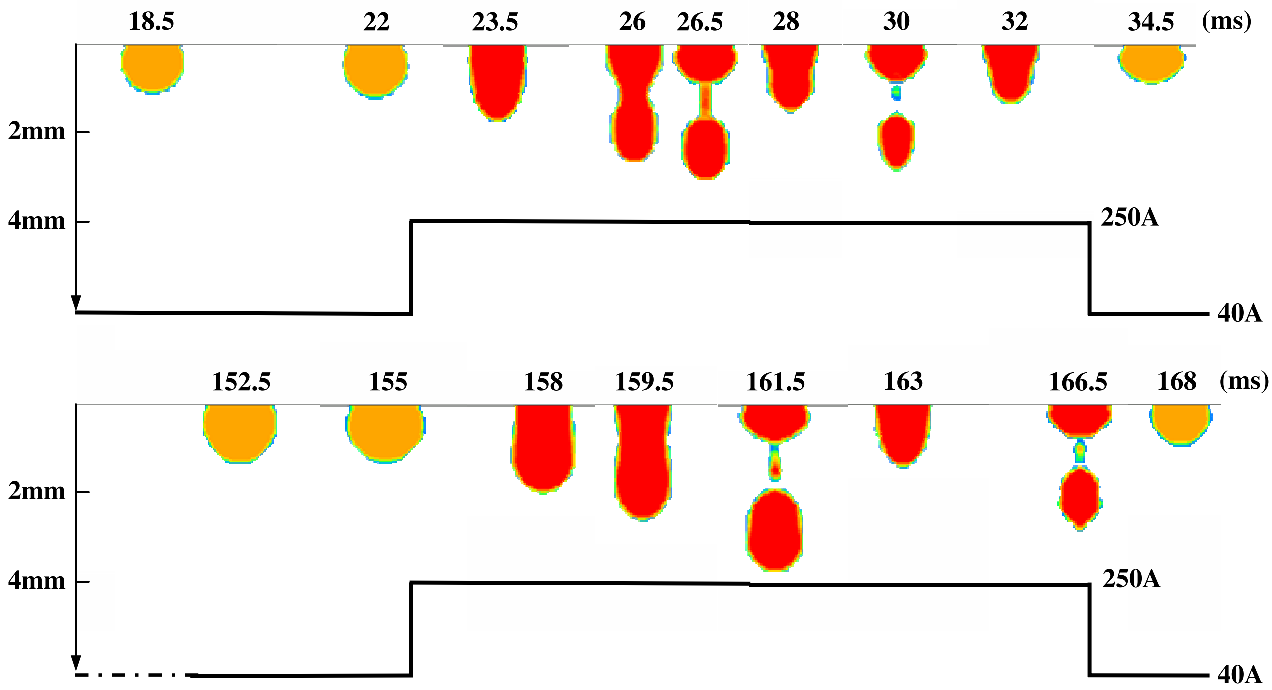

18.5
22
23.5
26
26.5
28
30
32
34.5
(ms)
2mm
4mm
250A
40A
152.5
155
158
159.5
161.5
163
166.5
168
(ms)
2mm
4mm
250A
40A

Figure 4(b)

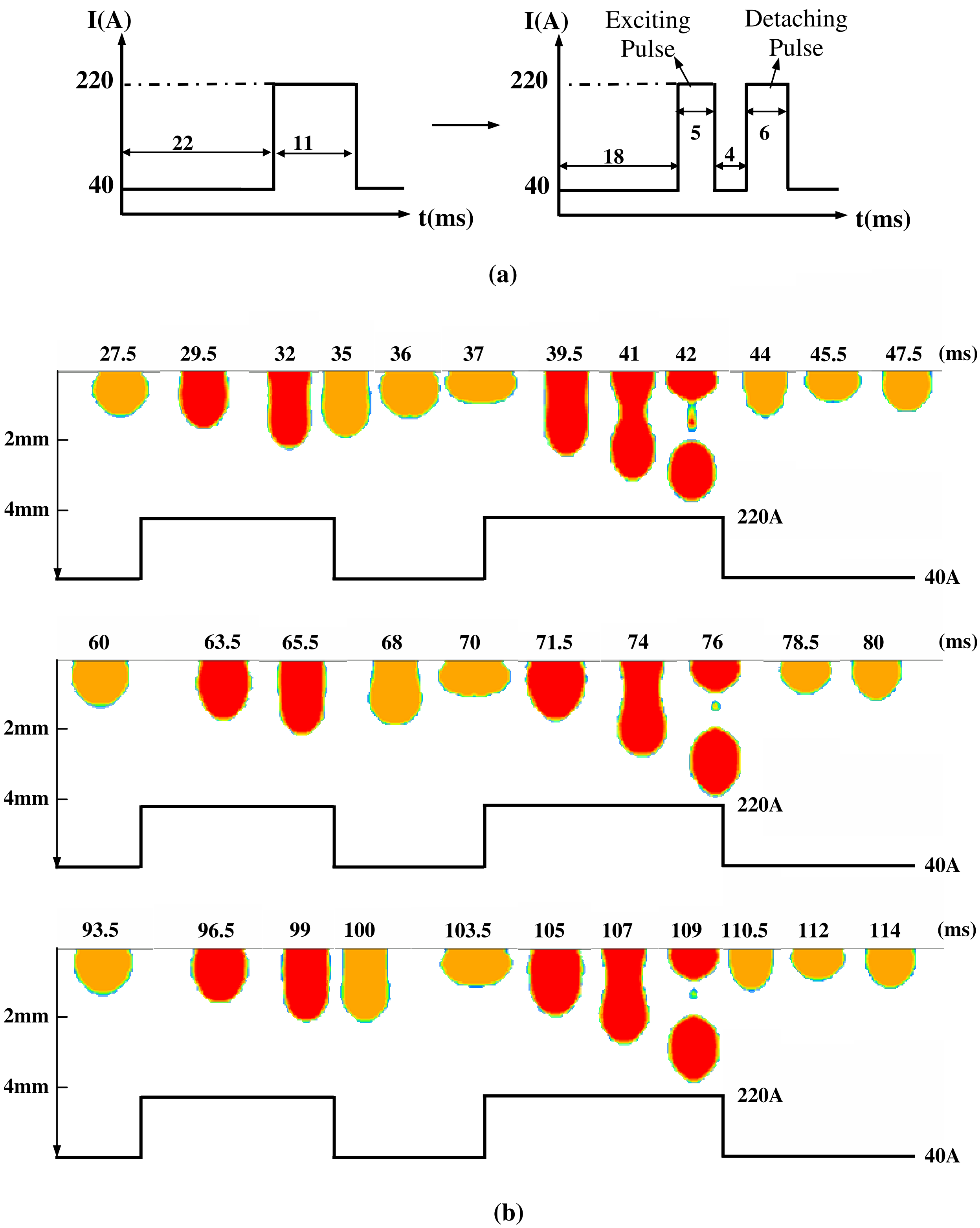
I(A)
220
40
22
11
t(ms)
I(A)
Exciting Pulse
Detaching Pulse
220
40
18
5
4
6
t(ms)
(a)
27.5 29.5 32 35 36 37 39.5 41 42 44 45.5 47.5 (ms)
2mm
4mm
220A
40A
60 63.5 65.5 68 70 71.5 74 76 78.5 80 (ms)
2mm
4mm
220A
40A
93.5 96.5 99 100 103.5 105 107 109 110.5 112 114 (ms)
2mm
4mm
220A
40A
(b)

Figure 5

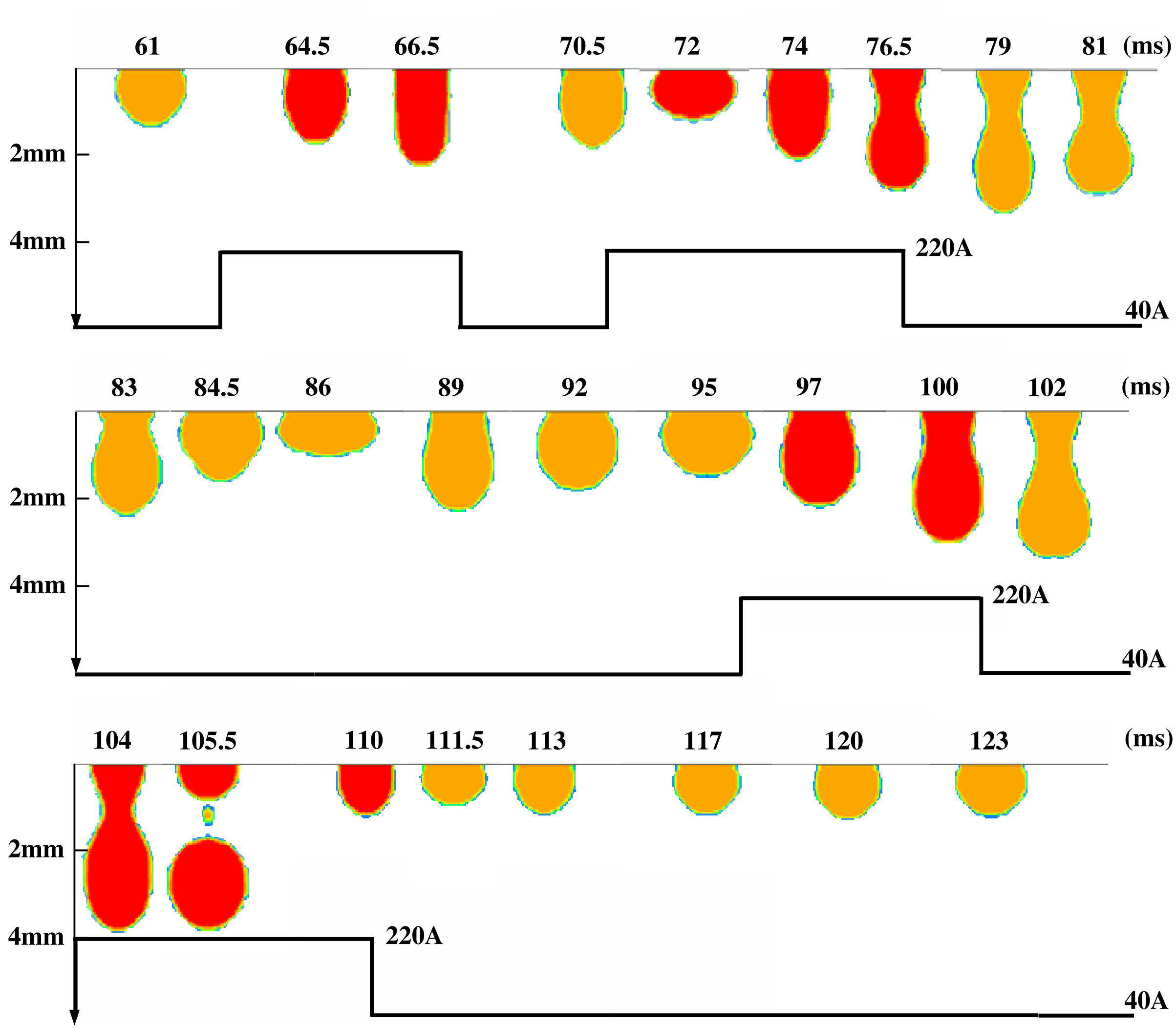
61
64.5
66.5
70.5
72
74
76.5
79
81
(ms)
2mm
4mm
220A
40A
83
84.5
86
89
92
95
97
100
102
(ms)
2mm
4mm
220A
40A
104
105.5
110
111.5
113
117
120
123
(ms)
2mm
4mm
220A
40A

Figure 6(a)

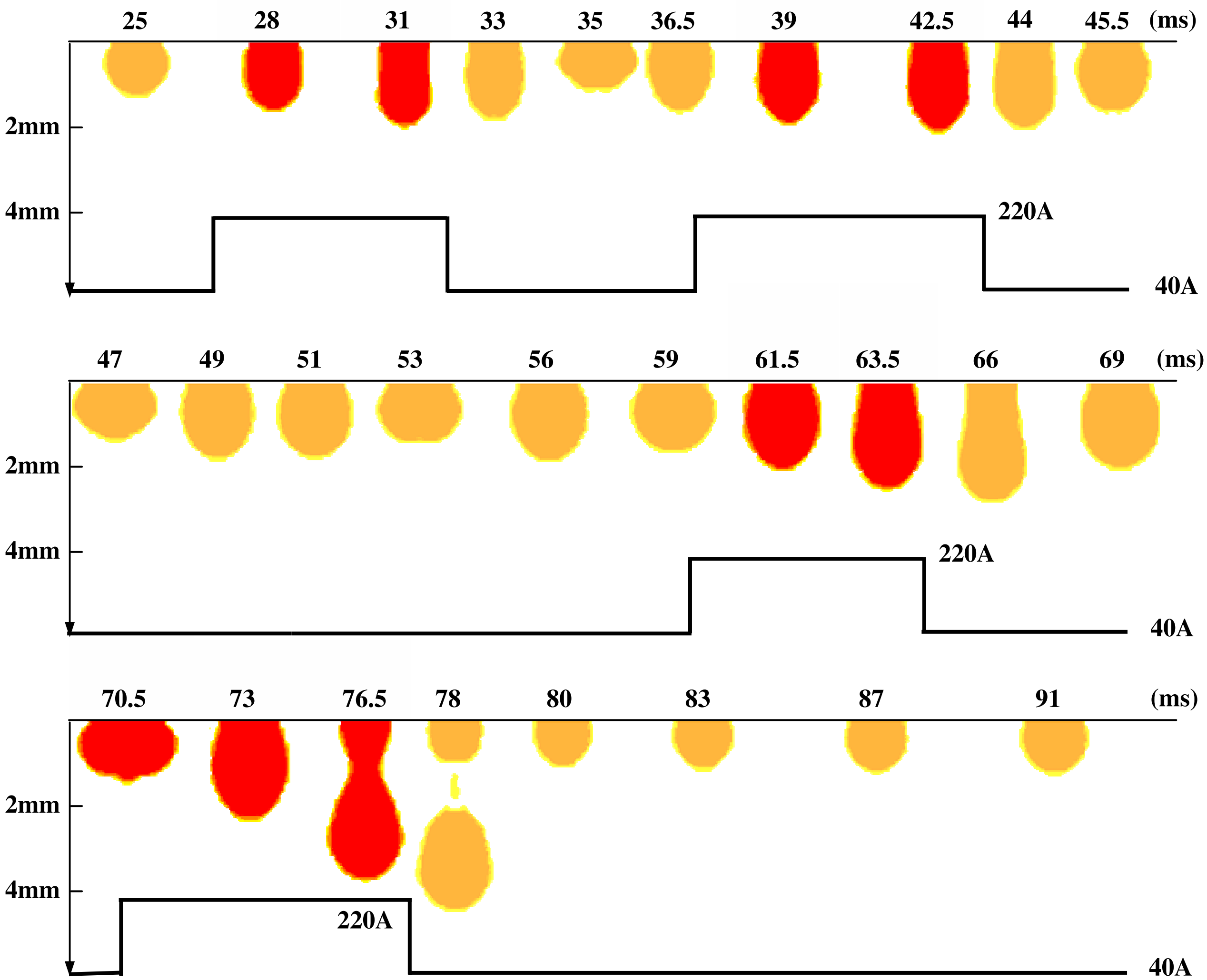
25
28
31
33
35
36.5
39
42.5
44
45.5
(ms)
2mm
4mm
220A
40A
47
49
51
53
56
59
61.5
63.5
66
69
(ms)
2mm
4mm
220A
40A
70.5
73
76.5
78
80
83
87
91
(ms)
2mm
4mm
220A
40A

Figure 6(b)

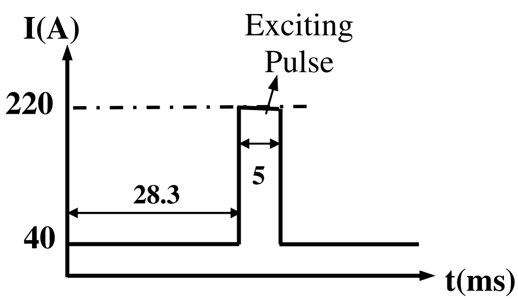

(a)

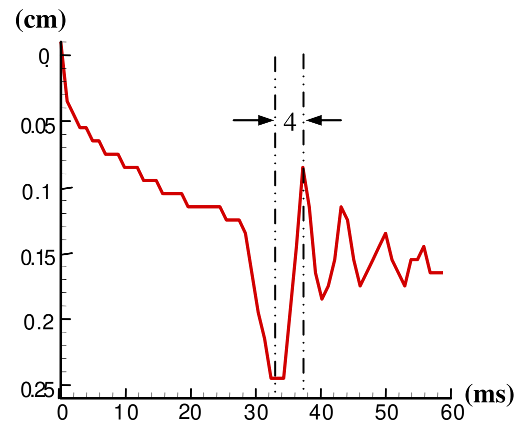

(b)

Figure 7

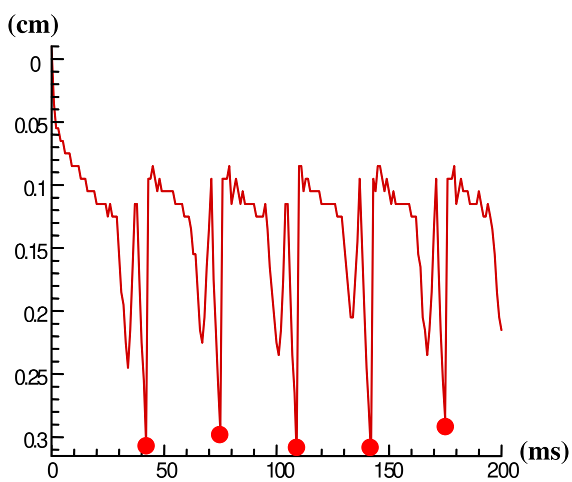

(a)

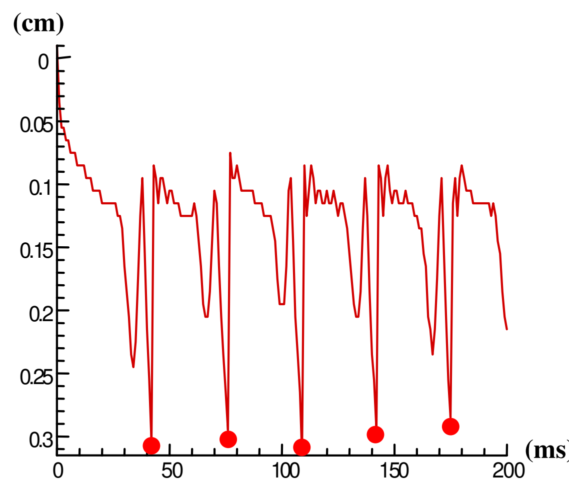

(b)

Figure 8

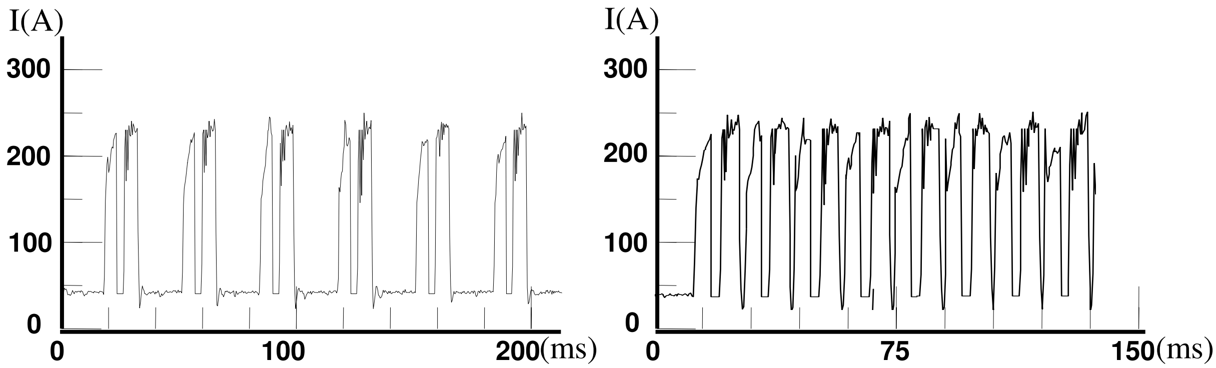

Figure 9(a)

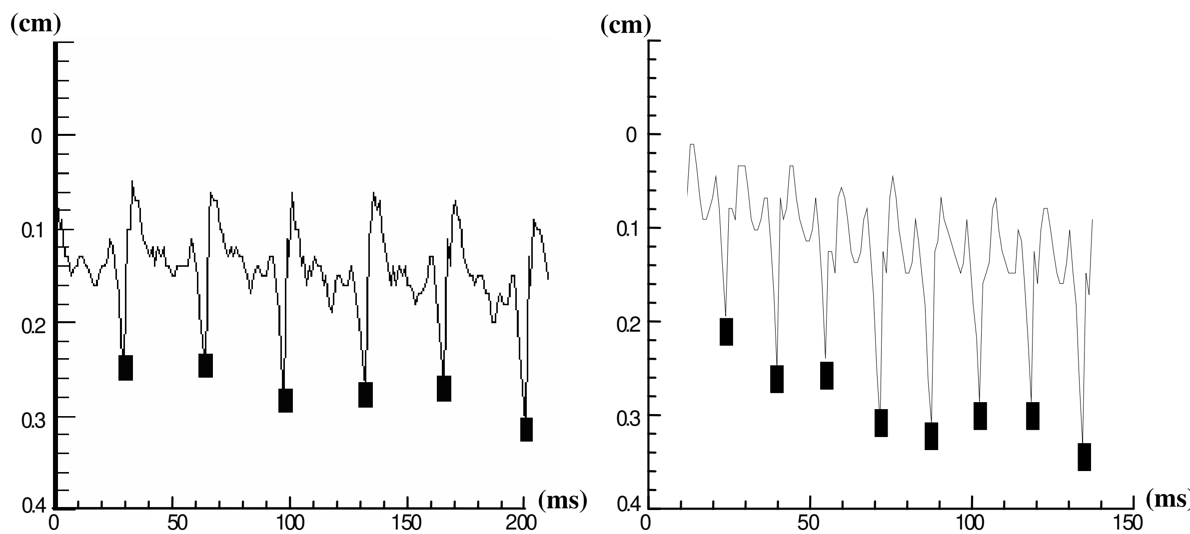

Figure 9(b)

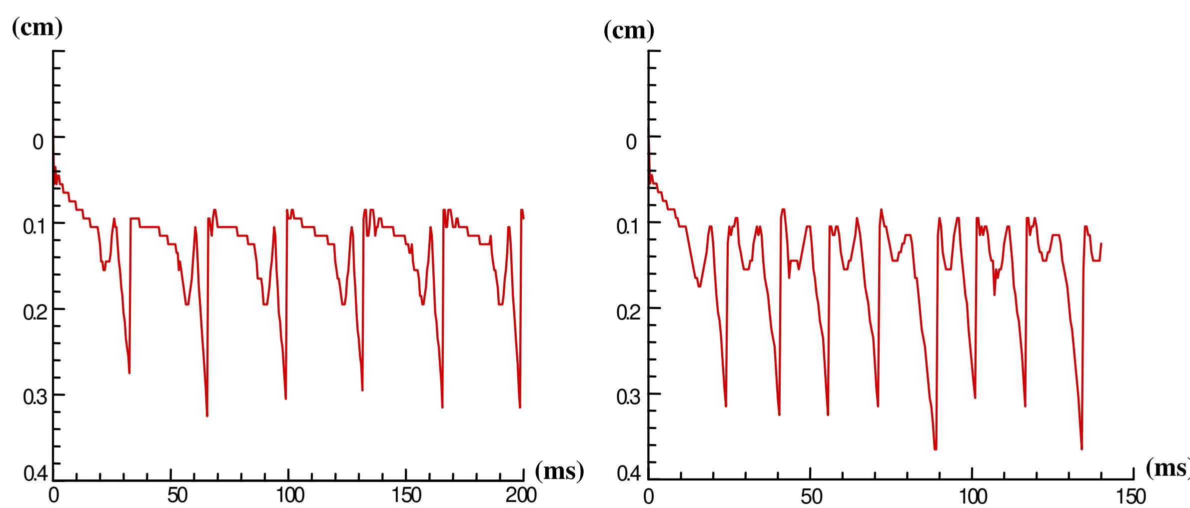

Figure 9(c)